Nucleic Acids Research

Supplemental Information

Organization of the human mitochondrial transcription initiation complex

Elena Yakubovskaya, Kip E. Guja, Edward T. Eng, Woo Suk Choi, Edison Mejia, Dmitri Beglov, Mark Lukin, Dima Kozakov, and Miguel Garcia-Diaz

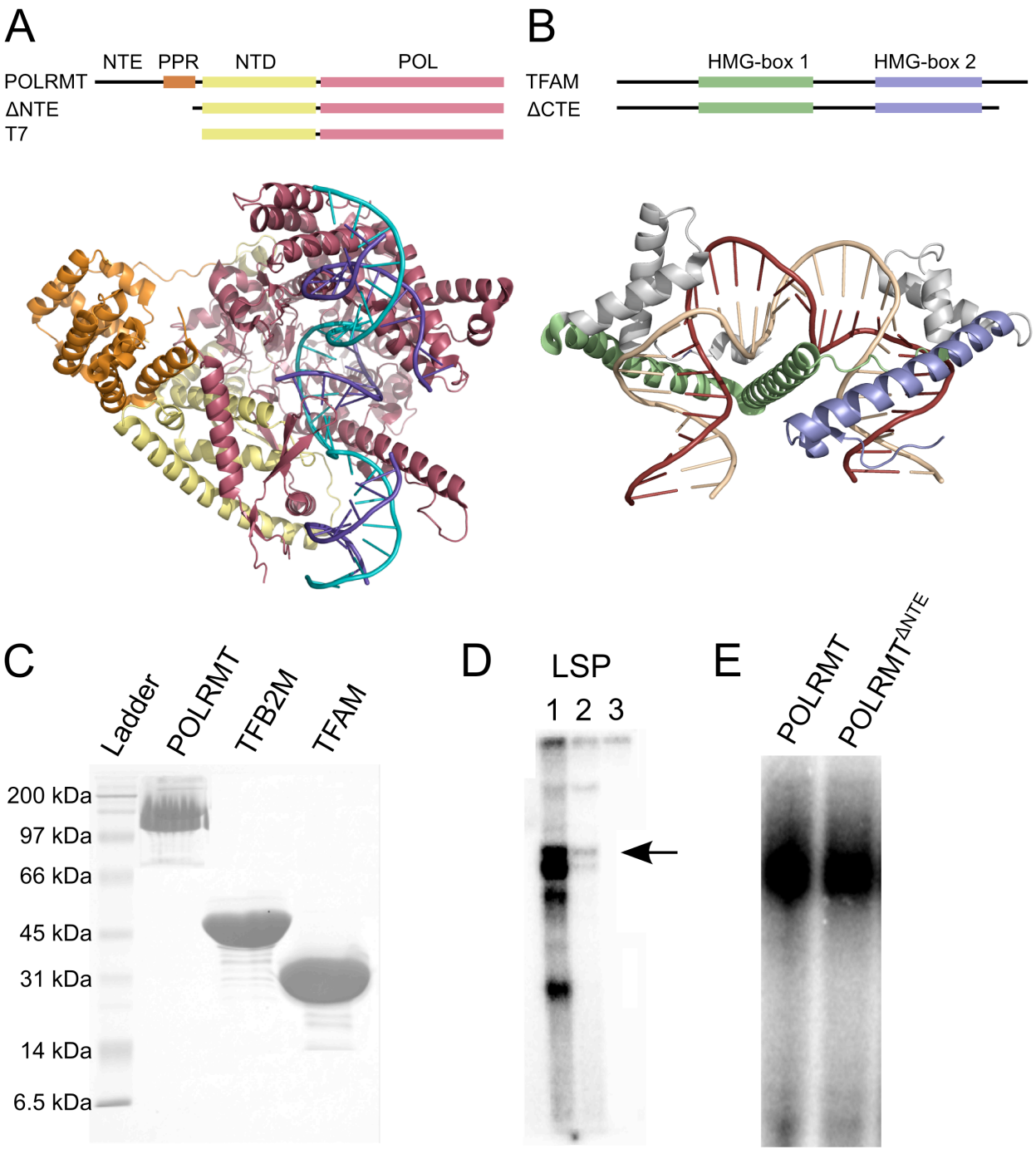

Supplementary Figure 1. Topology, purity, and activity of proteins used in this study.

(**A**). *Upper*. In addition to the polymerase domain and N-terminal domain present in T7 RNA polymerase, human mitochondrial RNA polymerase (POLRMT) contains a mitochondrial targeting sequence (residues 1–41) and a divergent N-terminal extension

(NTE) – a unique, flexible region of unknown structure (residues 42–217). A pentatricopeptide repeat (PPR; residues 218–368) is adjacent to the NTE (1). *Lower*. Crystal structure of the POLRMT elongation complex (2). (**B**)**.** TFAM contains two HMG-box domains followed by a short C-terminal tail. HMG-box domains are DNA-binding motifs that interact with the minor groove of DNA and in some cases, result in DNA bending (3,4). The bottom part of the figure shows the crystal structure of TFAM bound to the LSP TFAM binding site (4). (**C**). An SDS gel demonstrates that the purity of POLRMT, TFB2M and TFAM was 95-99%. The SDS-PAGE Molecular Weight Standards, Broad Range (BioRad) ladder was used and the molecular weights of the marker bands are labeled. (**D**). *In vitro* transcription assays from the mitochondrial light-strand promoter (LSP). In Lane 1, addition of POLRMT-FL, TFAM-FL and TFB2M resulted in robust initiation. In contrast, POLRMT$^{\Delta NTE}$ (Lane 2) or TFAM$^{\Delta CTE}$ (Lane 3) were incapable of promoting initiation in any of the experimental conditions tested. The run-off transcription product (300 bp) is indicated with an arrow. (**E**). Promoter-independent transcription from a substrate containing a 3′-protruding tail (tail-assay). Full-length POLRMT and POLRMT$^{\Delta NTE}$ are equally capable of promoting RNA synthesis.

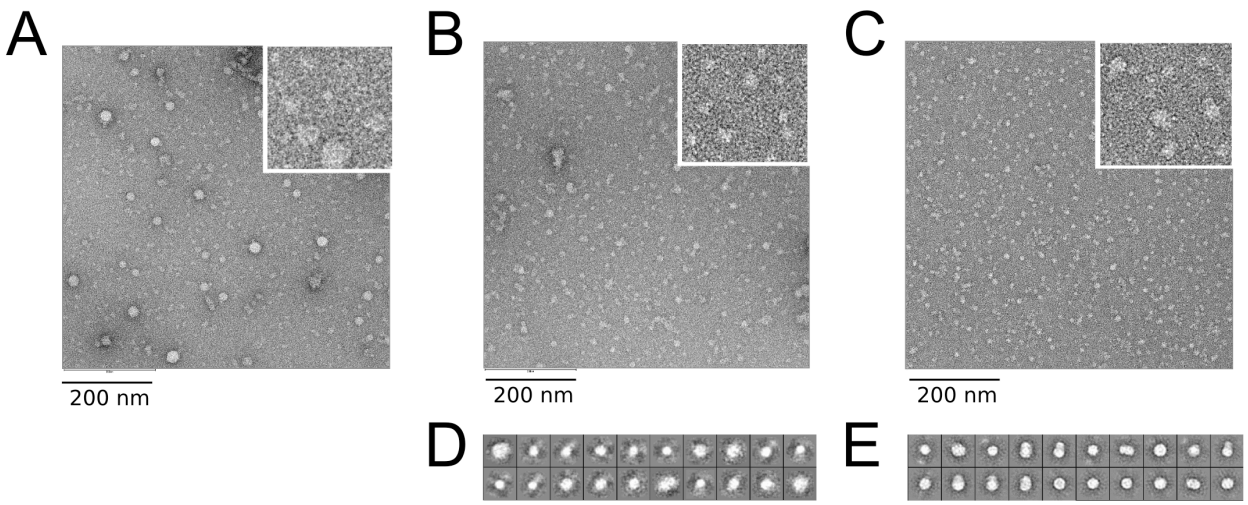

Supplementary Figure 2. Uranyl acetate stained electron microscopy grids. (**A**). Representative control grid prepared with a DNA fragment of arbitrary sequence (containing no promoter sequence) and the three full-length proteins (type A). (**B**). Representative control grid containing LSP DNA, POLRMT, TFB2M, and TFAM$^{\Delta CTE}$ (type B). (**C**). Representative grid with mitochondrial transcription initiation complex (POLRMT, TFB2M, TFAM), and LSP DNA (45bp; the same grid is shown in Figure 1A). Magnified insets are shown in the top right corner of each micrograph. (**D**). Reference free class averages obtained from a set of roughly 1400 individual images taken from type B grids. (**E**). Reference free class averages obtained from a set of roughly 4000 individual images taken from grids containing the mitochondrial initiation complex. Note: the high size variability of particles observed in type A grids precludes unbiased particle picking, and thus no reference free class averages could be produced for them.

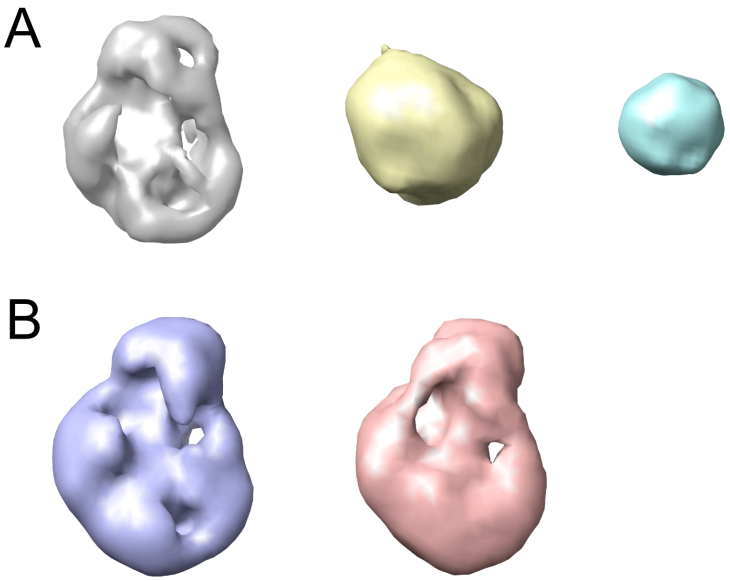

Supplementary Figure 3. Refinement of the mitochondrial initiation complex. (**A**). Initial models used for simultaneous refinement of the raw image set. *Left*. A model generated from larger class averages using the common line method. *Center*. A model generated from smaller class averages. *Right*. A random smaller size blob for capture of smaller fragments. (**B**). *Left*. An EM map obtained from the larger initial model (*top left*) after 20 cycles of iterative simultaneous refinement. *Right*. An improved model obtained after additional 20 cycles of refinement based on the selected image set.

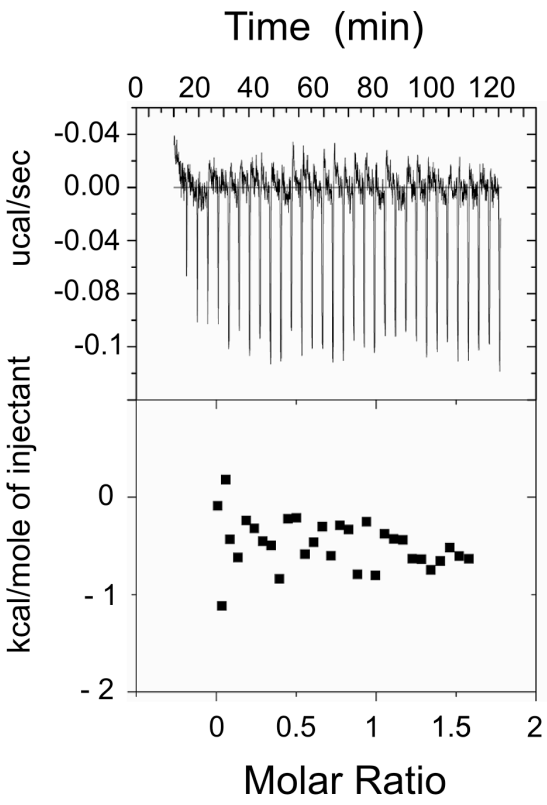

Supplementary Figure 4. Isothermal titration calorimetry experiments of TFB2M binding to POLRMT performed at 25 °C.

No thermal effect was observed for the putative interaction between TFB2M and POLRMT$^{\Delta NTE}$. The top panel represents the heat signal for injections of TFB2M into the calorimeter cell containing POLRMT. The bottom panel displays the integrated heat for each injection after peak integration and subtraction of basal values fitted to a simple single-site binding model (solid line).

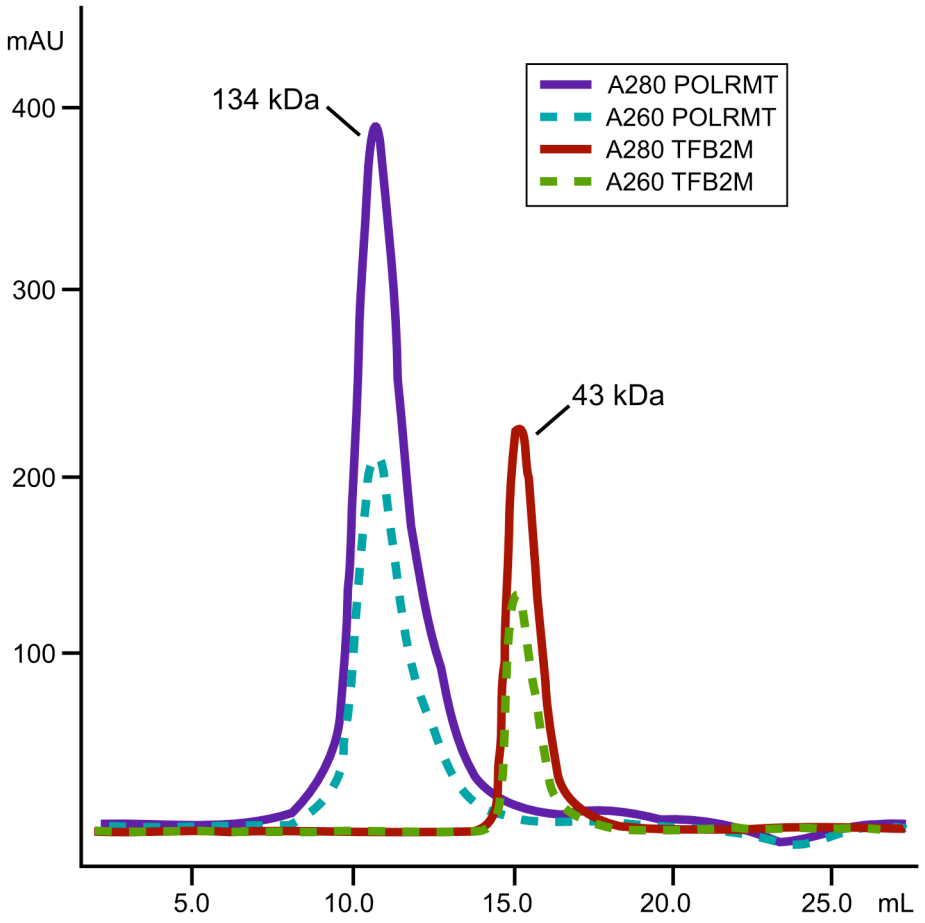

Supplementary Figure 5. Size exclusion chromatography of POLRMT and TFB2M. Elution profiles corresponding to the absorbance at 280 nm (A280; solid lines) and 260 nm (A260; dashed lines) are shown for each protein. Labels indicate the theoretical molecular mass predicted by amino acid sequence.

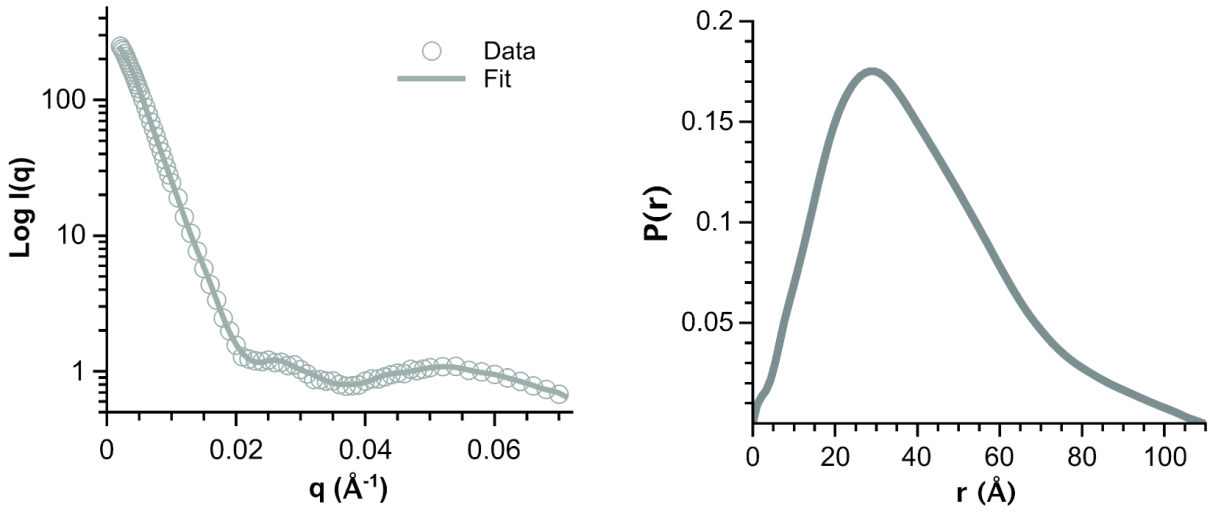

Supplementary Figure 6. Solution scattering data for human TFB2M.

Left. Experimental scattering-intensity data (circles) represented in a logarithmic scale as a function of the momentum transfer, $q = 4\pi \sin(\theta) \lambda^{-1}$ (2θ, scattering angle; λ = 0.9 Å, X-ray wavelength). Fit of the filtered average bead model is shown as a solid line. *Right*. Pairwise distance distribution function, *P*(r). The calculated maximal dimension, D_{max}, and radius of gyration, R_g were 109 Å and 35.8 ± 1.0 Å, respectively.

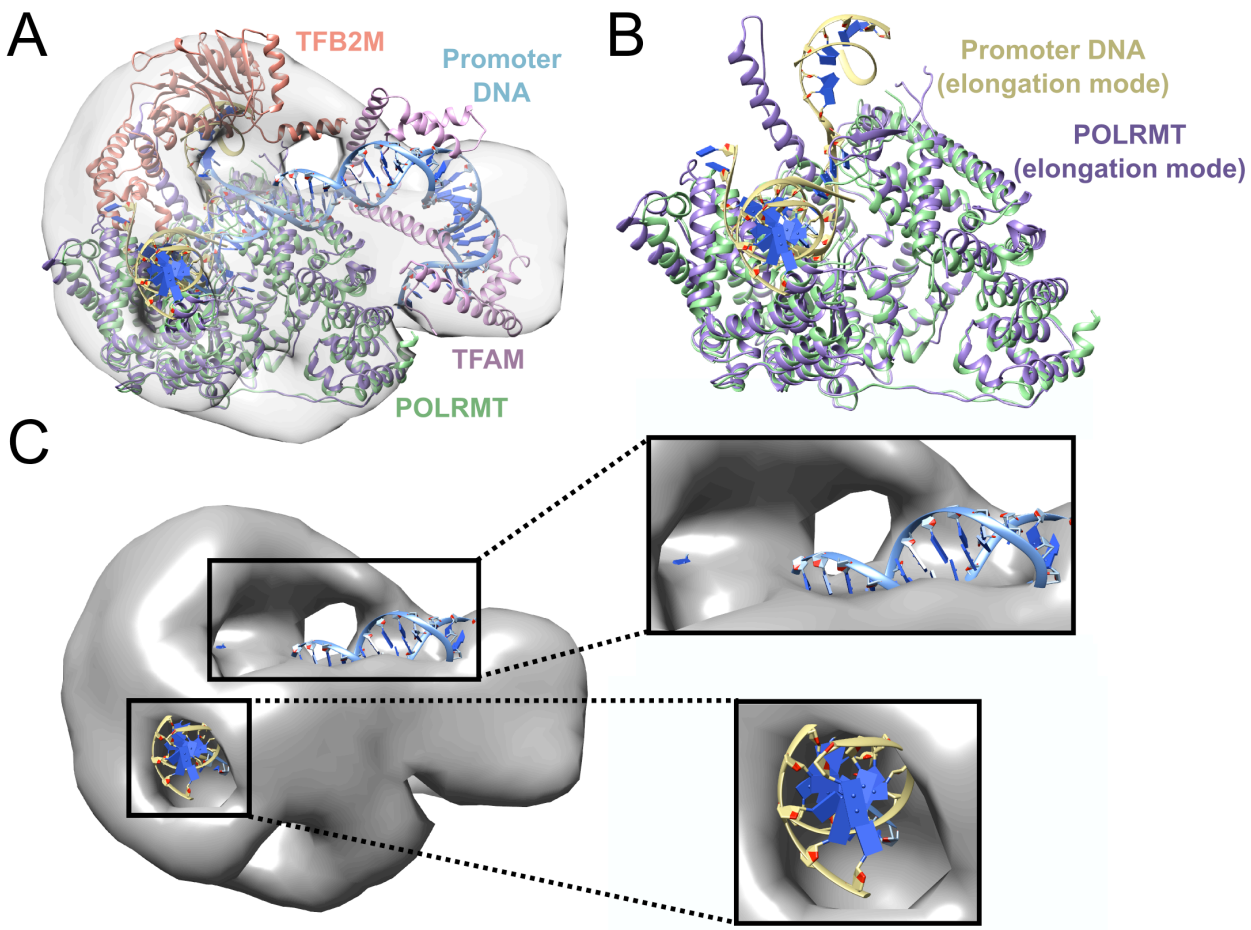

Supplementary Figure 7. Model of the initiation complex superimposed on the crystal structure of the POLRMT elongation complex.

(**A**). The EM envelope for the full complex is shown as a grey transparent surface, while POLRMT, TFAM, TFB2M and the promoter DNA are shown as ribbons colored green, purple, orange, and blue respectively. (**B**). The crystal structure of the POLRMT elongation complex (2) has been superimposed on the POLRMT molecule in the initiation complex. (**C**). Close inspection of the EM map reveals a clear groove for the DNA, which unlike proteins appears almost invisible on negatively stained EM grids. Insets show detail of entry and exits points for the DNA.

Supplementary References

1. Arnold, J.J., Smidansky, E.D., Moustafa, I.M. and Cameron, C.E. (2012) Human mitochondrial RNA polymerase: structure-function, mechanism and inhibition. *Biochimica et biophysica acta*, **1819**, 948-960.
2. Schwinghammer, K., Cheung, A.C., Morozov, Y.I., Agaronyan, K., Temiakov, D. and Cramer, P. (2013) Structure of human mitochondrial RNA polymerase elongation complex. *Nature structural & molecular biology*, **20**, 1298-1303.
3. Rubio-Cosials, A., Sidow, J.F., Jimenez-Menendez, N., Fernandez-Millan, P., Montoya, J., Jacobs, H.T., Coll, M., Bernado, P. and Sola, M. (2011) Human mitochondrial transcription factor A induces a U-turn structure in the light strand promoter. *Nature structural & molecular biology*, **18**, 2081-1289.
4. Ngo, H.B., Kaiser, J.T. and Chan, D.C. (2011) The mitochondrial transcription and packaging factor Tfam imposes a U-turn on mitochondrial DNA. *Nature structural & molecular biology*, **18**, 1290-1296.